



Depletion of sulfur on the surface of asteroids and the moon

R. M. KILLEN

University of Maryland, Department of Astronomy, College Park, Maryland 20742, USA
E-mail: rkillen@astro.umd.edu

(Received 29 July 2002; revision accepted 14 December 2002)

Abstract—Data from the X-ray and γ -ray spectrometers onboard the Near Earth Asteroid Rendezvous (NEAR) spacecraft were used to constrain the chemical and mineralogical composition of asteroid 433 Eros (McCoy et al. 2001). The bulk composition appears to be consistent with that of L to H chondrites (Nittler et al. 2001). However, there appeared to be a marked depletion relative to ordinary chondritic composition in the S/Si ratio (0.014 ± 0.017). We investigate space weathering mechanisms to determine the extent to which sulfur can be preferentially lost from the surface regolith. The two processes considered are impact vaporization by the interplanetary meteoroid population and ion sputtering by the solar wind. Using impact data for Al projectiles onto enstatite, we find that the vaporization rate for troilite (FeS) is nine times as fast as that for the bulk of the regolith. If 20% of the iron is in the form of troilite, then the net vaporization rate, normalized to bulk composition, is 2.8 times faster for sulfur than for iron. Sputtering is equally efficient at removing sulfur as impact vaporization.

INTRODUCTION

Data from the X-ray and γ -ray spectrometers onboard the Near Earth Asteroid Rendezvous (NEAR) spacecraft were used to constrain the chemical and mineralogical composition of asteroid 433 Eros (McCoy et al. 2001). Abundances for major and geologically important elements Mg, Al, Si, S, Ca, and Fe were determined from NEAR X-ray γ -ray spectrometer (XGRS) measurements of the X-ray spectrum of the asteroid taken during major solar flares. Although the bulk composition of Eros appears to be consistent with that of L–H chondrites, S was not detected. The detection limit for S should be approaching a couple of tenths of a percent during a solar flare. Thus, the nondetection of S with the XGRS is significant (Nittler et al. 2001). We conclude that S is depleted on the extreme surface of Eros by an order of magnitude relative to ordinary chondrite S abundances. In contrast, the Fe/Si ratio found from the XGRS data is larger than that expected for L–H chondrites. The marked depletion relative to ordinary chondritic composition in the S/Si ratio (0.014 ± 0.017) lead researchers to question the assumption that the composition of the extreme surface probed by the X-ray and γ -ray spectrometers (upper 100 μm and upper tens of cm, respectively) is representative of the underlying bedrock.

Loss of volatiles occurs from the extreme surface of airless bodies such as the moon, Mercury, and planetary satellites by processes such as impact vaporization, photo-

sputtering, and ion-sputtering, followed by Jeans escape or ionization and entrainment in the solar wind (e.g., Killen et al. 2001). However, on a small body such as Eros, with an escape velocity of 3–17 m s^{-1} , all of the vaporized species will immediately thermally escape. In fact, all vaporized sulfur will have a velocity greater than the escape velocity if the impact vapor has a 5000 K Maxwellian velocity distribution (Sugita, Schultz, and Adams 1998), compared with 23% at the moon and 0.3% at Mercury.

Impact vaporization and outgassing have led to enrichment of volatiles in the lunar regolith, particularly Rb, Cs, U, and ^{40}Ar (Haskin and Warren 1991), rather than a net loss, because expansion velocities are less than escape velocity. Thus, the question for selective devolatilization at asteroids is this: what volume of the target surface is raised to a temperature at which the most volatile species will vaporize but the refractory species will not?

Energy partitioned to target heating increases as $\cos^2(\theta)$ for the impact angle θ measured from the horizontal. If θ is the impact angle measured from the horizontal, the vapor temperature increases as $v_i \sin \theta$, from a minimum angle of 15° (Sugita, Schultz, and Adams 1998), where v_i is the impact velocity. This means that vaporization is more efficient for low impact angles, but the vapor can come off at a lower temperature (Schultz and Gault 1989). This has profound implications for atmospheric escape, but may have less impact on escape from asteroids than from the moon and the planets.

One important observation is that, although volatiles in general are enhanced in lunar glasses, sulfur is depleted, as it is on Eros. Troilite-rich regions in H chondrite breccias have been cited as evidence for impact-vaporization of sulfide on OC asteroids (Rubin 2002). Some of the sulfur vapor that reimpacts the surface will condense into fractures as S_2 , where it will scavenge Fe to form FeS (Rubin 2002). This process may have occurred at the moon as well. Enhancement of iron on the surface of Eros could be additional evidence of outgassing, which has been shown to bring small grains of iron to the surface in a microgravity environment (Sears et al. 2002).

Alteration of the composition of basalt melts has been observed in terrestrial impact craters and attributed to selective vaporization (Parfenova and Yakovlev 1977). The vaporization pattern is a function of the composition of the mineral as a whole, being dependent on the activity in the melt.

CALCULATIONS

Impact Vaporization

We use the impedance matching method to calculate the rate of impact vaporization (Melosh 1989; Morgan and Killen 1998). For completeness, we reiterate these equations here.

The peak pressure, P_p , in the target material due to an impactor with initial impact velocity, v_i , is:

$$P_p = (\rho v_i^2/4)(2C/v_i + S) \quad (1)$$

where C is a constant close to the bulk speed of sound in the medium and S is an empirical constant related to the physical properties of the target, such as volume coefficient of expansion, bulk modulus, and specific heat (Morgan and Killen 1998). Values of C and S appropriate for various minerals are given in Melosh (1989) Appendix II. The values that we used in this study are reproduced in Table 1. P_p is in Pascals if v_i is in m/s. The pressure, $P(R)$, decays with radius from the impact center, R , as:

$$P(R) = P_p(R/r_0 - c)^{-(avi + b)}, \text{ for } R/r_0 > c \quad (2)$$

where a and b are 0.052 s/km and 1.19, respectively, for anorthosite (An) onto anorthosite impacts and 0.0825 s/km and 1.24 for Fe onto An (Lange and Ahrens 1982). This gives a decline in pressure between that expected for low pressure as $r^{-3/2}$ and that for high pressure as r^{-3} (Melosh 1989). The mass vaporized is that mass inside the radius, R_{cp} , where the pressure $P(R_{cp}) = P_{cp}$, the critical pressure for vaporization. The parameter c is the scaled radius at the onset of far field attenuation and varies between 2 and 3 (Lange and Ahrens 1982). We use a value of 2 because it agrees better with the data than a higher value (Lange and Ahrens 1982). The radius, r_0 , defines the volume into which the initial energy is placed and is assumed to be equal to the projectile radius.

The peak pressure increases with distention because porous materials are less efficient at transmitting energy through shocks. Thus, the impact energy is deposited in a smaller area. We scale P_p for the distention, m , of the regolith:

$$P_p(m) = 1.2P_p(1)(m + 0.05)^{3.6} \quad (3)$$

(Morgan and Killen 1998) and the distention, m , is related to porosity, p , by:

$$m = 1/(1 - p) \quad (4)$$

The distention for the lunar regolith is between 1.8 for the upper tens of cm and 1.1–1.2 to a depth of 1 km (Lange and Ahrens 1982). We use a distention of 1.8, or a porosity of 0.4, because most of the impactors are small and will affect only the uppermost regolith. However, our code does not properly handle distention in general. The vaporization rate increases with porosity as shown in Table 4. Now, to obtain the mass vaporized as a function of impactor mass, we simply solve for $R(P_{cp})$. The volume being vaporized is $4/3\pi R^3$. We first define a normalized radius, s , the radius of the devolatilized region in units of impactor radius:

$$s(P_{cp}) = R(P_{cp})/r_p \quad (5)$$

Then we simply ratio the vaporized volume to the volume of the impactor, $4/3\pi r_p^3$, and given the relative densities, we obtain the vaporized mass in units of impactor mass:

$$m_{\text{vap}}/m_{\text{pr}} = \rho_{\text{reg}}/(2\rho_{\text{impactor}})(s[P_{cp}])^3 \quad (6)$$

where $m_{\text{vap}}/m_{\text{pr}}$ is the ratio of the vaporized mass to the mass of the projectile, given the relative densities, ρ_{reg}/ρ_p . The factor of 0.5 results from the fact that only a hemisphere of regolith is vaporized rather than a full sphere. Inverting Equation 2 for $P(R_{cp})$ to obtain the radius that just reaches critical pressure for vaporization, we obtain:

$$s_{cp}(v_i) = \{P_p(v_i)/P_{cp}\}^{-(avi + b) + c} \quad (7)$$

Now, to obtain the total mass vaporized by the incoming meteor population, we integrate Equation 6 over the velocity distribution of incoming micrometeoroids translated to the orbital distance of the asteroid, r AU (Cintala 1992, Equations A11–A12):

$$f(v_r) = k \cdot r^{0.2} \left(\frac{v_r}{\sqrt{r \cdot v_r + [v_E]^2}} \right)^3 \exp^{\gamma \sqrt{r \cdot (v_r)^2 + (v_E)^2}} \quad (8)$$

where $f(v_r)$ is the velocity distribution for r AU adjusted for changes in the spatial distribution of particles. The constants, k and γ , are 3.81 and 0.247 (s km⁻¹), respectively, and the velocities, v_r and v_E , are the impact velocity at the asteroid and the escape velocity for the Earth at 100 km altitude (11.1 km s⁻¹), respectively. The peak in the impact velocity probability function at Eros, plotted in Fig. 1, is near 9 km s⁻¹, close to the minimum velocity required to vaporize the target. In contrast,

Table 1. Equation of state parameters.

Material	ρ_0 (kg/m ³)	C (km/s)	S
Anorthosite	–	7.71	1.05
Al	2750	5.30	1.37
Diabase	3000	4.48	1.19
Iron	7680	3.80	1.58
Calcite	2670	3.80	1.42
Quartz	2650	3.68	2.12
Basalt	2860	2.60	1.62
Dry sand	1600	1.70	1.31
Regolith	1800	1.28	1.56
Ice (0°C)	910	1.28	1.56

Table 2. Enthalpy of vaporization for various minerals, metals, and oxides.

Material	Enthalpy of vaporization (MJ/kg)
FeS	1.150
Fe	6.272
Diabase	8.500
Regolith	9.643
MgO	10.46
SiO ₂	20.93

the mean impact velocity at Mercury is 20 km s⁻¹ (Cintala 1992).

In our previous calculations (Morgan and Killen 1998; Killen et al. 2001), we assumed that the critical pressure for vaporization was the pressure at which the target is completely vaporized. However, the temperature at which the liquid is completely converted to vapor is the highest temperature of vaporization of the constituent oxides or gases that boil off. The temperature at which a given constituent vapor boils off a mineral is the temperature of vaporization of the individual component (Ahrens and O'Keefe 1972). Thus, the more volatile components will vaporize first, at significantly lower impact velocities, than those required for complete vaporization.

We estimate the critical pressure for vaporization of individual gases by scaling the critical pressure for vaporization of regolith, as defined by Cintala (1992), by the ratio of the enthalpies required for vaporization (Chase et al. 1985), given in Table 2. This scaling is approximate but will result in a reasonable estimate of relative loss rates. Other factors also influence the volatility of individual species: density, porosity, and concentration of the volatile species. We have included these factors in our solution.

A species with an initially low concentration resists vaporization, but this factor is not considered in these results. Vaporization may be enhanced in vacuum conditions, especially important for medium volatility components such as FeO. Since we use thermodynamic values measured at atmospheric pressure, the exact vaporization rate at vacuum is not duplicated.

The critical pressure for complete vaporization of regolith was calculated by Cintala (1992) to be 236 GPa. The

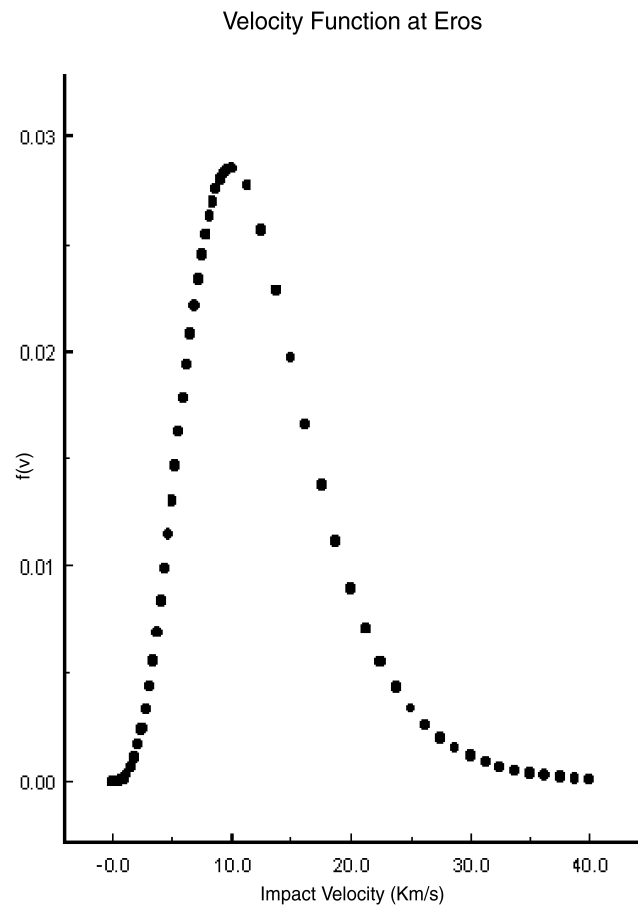


Fig. 1. The probability function for impact velocity, v (km s⁻¹), at Eros at an orbital distance 1.34 AU using Equation 8.

thermodynamic properties of “regolith” used in this paper are those defined by Cintala, which include a linear fit to the shock-particle velocity relationship for lunar regolith 70051 and a second fit at higher shock velocities derived from Nevada Test Site basalt.

Because of its much smaller enthalpy of vaporization, troilite (FeS) will vaporize at about 102 GPa. This is somewhat larger than the pressure at onset of vaporization (as opposed to the complete vaporization) for lunar regolith. We will determine the total amount of vaporization of S and Fe by assuming that all of the sulfur and one fifth of the iron reside in troilite, FeS. This is somewhat higher than the percentage of iron residing in troilite in the lunar highlands (16%) (Haskin and Warren 1991). We will assume that the iron not residing in FeS resides in more refractory minerals and will vaporize with the refractory portion of the regolith. Thus, the critical pressure for total vaporization of iron not residing in FeS is assumed to be 236 GPa.

The total vapor produced will be sensitive to the minimum impact velocity required to vaporize a particular constituent. This follows from the fact that the peak of the velocity distribution for meteoroids is about 9 km/s at Eros orbit, while the minimum velocity required for complete

vaporization is 8.8–14 km/s (Ahrens and O’Keefe 1972). The amount of vaporization and the minimum impact velocity required for vaporization is a function not only of composition and bulk density, but also of distention, m , where m is defined as the volume of the porous material to the initial crystal volume. We fit data for v_{\min} as a function of distention for Al and Fe projectiles onto enstatite and dunite, respectively (Ahrens and O’Keefe 1972), as given in Table 3.

Our function for the minimum impact velocity required for vaporization has the form of a quadratic:

$$v_{\min} = a + b \cdot m + c \cdot m^2 \quad (9)$$

where the constants a , b , and c are given in Table 3 as a function of rock type and impactor type. Aluminum was chosen as the impactor because the properties of aluminum are closest to those of stony-iron meteorites, and it has been used in many lab tests.

However, devolatilization begins at much lower pressures than that required for complete volatilization. The critical pressure for complete vaporization of regolith, calculated by Cintala (1992), is 236.1 GPa, while that required for the onset of vaporization is 39.06 GPa. Thermodynamic constants assumed for “regolith” are given in Cintala (1992) Table 1. If we scale the critical pressure for volatilization by the enthalpy of vaporization and assume that the volume density is the same for both species, we find that the critical pressure for complete devolatilization of FeS will be 102.5 GPa, while the pressure for the onset of volatilization of FeS will be 16.96 GPa. Vaporization of anorthosite begins at much higher pressures: incipient vaporization occurs upon release from shock pressures of 120 GPa (Jeanloz 1979). This pressure agrees with that found by Boslough and Ahrens (1983) for gabbroic anorthosite, but a slightly lower pressure of 92.4 GPa was found for incipient vaporization of anorthite glass (as expected) (Boslough and Ahrens 1983).

The temperature of the vapor will be lower the closer the impactor velocity becomes to the minimum velocity required to vaporize the target (Ernst and Schultz 2002). In addition, the temperature of the vapor increases as $\sin(\theta)$, where θ is the impact angle measured from the horizontal (Schultz 1996).

The data in Sugita, Schultz, and Adams 1998, were fit to a function of x where $x = v_i \sin \theta$. The temperature of the vapor, T , is $T = (2000x + 7000)/3$. This results from the fact that as impact angles decrease, a larger fraction of the impactor energy is carried off by the downrange impactor debris.

The mean velocity of expansion of a vapor cloud created from a hyper-velocity impact is twice the sound speed in the medium regardless of the impact velocity. For regolith, the sound speed is about 1.3 km/s. Thus the expansion velocity is on the order of 2 km/s (Schultz 1996). The expansion velocity is comparable to the lunar escape velocity, 2.38 km/s, but much higher than the escape velocity from Eros (17 m/s). The only reasonable way to preferentially lose one species rather

Table 3. Parameters to fit the minimum impact velocity as a function of distention.

Mineral	a	b	c
Al—Enstatite	21.014	-14.154	3.058
Al—Dunite	28.214	-27.23	7.812
Fe—Enstatite	16.657	-11.371	2.5
Fe—Dunite	18.893	-17.034	4.866

than another on the surface of an asteroid is to preferentially vaporize that species. At Mercury and the moon, prompt escape is very unlikely.

Although a large amount of vapor is produced by oblique impacts, partly because more area is impacted by the incoming meteorite, the vapor comes off relatively cool. A simple relationship between the mass of the vapor, m_v , mass of projectile, m_p , and the impactor velocity, v , and angle, θ , is:

$$m_v/m_p = v^2 \cos^4 \theta \quad (10)$$

for angles between 7.5° and 45° (Schultz 1996). For dry ice targets, the vaporized target mass increases by two orders of magnitude as the impact angle decreases from 45° to 15°, but for carbonate targets, it increases by a more modest factor of about 20. We have fit the data for the vaporization of dolomite targets as a function of impact angle (Schultz 1996) and integrated this function over the probability function for impacts at angles from the horizontal of 0 to $\pi/4$. We take the probability of impact at angle θ from the horizontal to be proportional to $\sin(2\theta)$ (Shoemaker 1962). This results in an increase by a factor of 12.6 over the vaporization calculated for vertical impacts.

The calculations are from the impedance matching method (Melosh 1989), with corrections for oblique impacts. Our results were checked against the vaporization rate found by Boslough and Ahrens (1983) for anorthosite impacting onto anorthosite, where an anorthosite impactor at 15 km/s vaporized 5 times its mass. Although 50 times the impactor mass reached critical pressure, only 10% of that material was vaporized. In addition, not all of the vaporized material reached the surface. We also compared our total vapor rate with that obtained using a fit to hydrocode calculations of the volume of melt plus vapor (Pierazzo, Vickery, and Melosh 1997), with constants given in their Table 4. For our “regolith” with zero porosity, our results are thirty percent larger than their results for granite. With a porosity of 0.5, our vaporized mass for “regolith” is half their vaporized mass for ice but ten times that for their “all data, no ice” case. However, the materials, other than ice, in their work (dunite, granite, aluminum and iron) require higher pressures for complete vaporization than our “regolith.” For example, the pressure required to completely vaporize dunite is 2220 GPa, almost ten times that required to vaporize regolith (236 GPa).

Lange and Ahrens (1982) define a dehydration efficiency for loss of water due to impacts, but do not make a quantitative estimate of its magnitude. For this reason, we did

Table 4. Vaporization rate per 1% abundance for S and bulk regolith.

Density (kg/m ³)	Porosity	Ratev (S) (atom cm ⁻² s ⁻¹)/1%	Ratev (reg) (atom cm ⁻² s ⁻¹)/1%
1800	0.5	1.3 E7	1.1 E6
1800	0.4	5.5 E6	6.0 E5
1800	0.3	2.8 E6	3.8 E5
3000	0.5	2.2 E7	1.8 E6
3000	0.4	9.2 E6	9.9 E5
3000	0.3	4.6 E6	6.2 E5

not include the factor of 12.6 increase in vaporization due to oblique impacts. In effect, our “dehydration efficiency” is about 10%.

Ion Sputter

Sulfur can be depleted from a surface by sputtering from solar wind plasma. If the yield of sulfur is similar to that of sodium, then we can expect a yield of about 0.08 per incident proton in the energy range of 500 eV up to 2 keV (Lammer et al. 2002). An average solar wind proton has an energy of about 800 eV. If the solar wind density is 100 cm⁻³, the velocity is 400 km s⁻¹, and the sulfur fraction in the regolith is 1%, the yield of sulfur will be approximately 3 × 10⁶ cm⁻² s⁻¹. This yield is comparable to the yield from impact vaporization at a density of 1800 kg m⁻³ and porosity of 0.3. Since ion sputter is much less effective for refractory materials, then it is more effective at selective depletion of volatiles, especially on bodies which are constantly exposed to the solar wind.

CONCLUSIONS

Using the values for impact of Al onto enstatite, we find that the vaporization rate for troilite is 9 times faster than that for the bulk of the regolith. Our vaporization rate is consistent with that given in our previous estimate for the same conditions (bulk regolith, $\rho = 1.8$ g/cm³, porosity = 0.4) (Clark et al. 2001).

If 1/5 of the iron vaporizes with the troilite (iron sulfide), then the loss rate for iron, normalized to the composition, is 29% that of sulfur. This is consistent with a relative sulfur depletion found for Eros by the Near Earth Asteroid Rendezvous (NEAR) X-ray and γ -ray spectrometers (McCoy et al. 2001).

If hyper-velocity impacts create a gas at about 5000 K (Sugita, Schultz, and Adams 1998), then we find by integrating the Maxwellian velocity distribution from the escape velocity to infinity that all of the hot sulfur will escape from an asteroid the size of Eros, but 23% will escape from the moon, and 0.3% will escape from Mercury. (If sulfur is in the form of S₂, then only 4% will escape from the moon and virtually none from Mercury). Some of the volatiles that remain in the atmospheres of Mercury and the moon will be

photoionized. However, the loss of ions by entrainment in the solar wind is not complete, even at the moon which is devoid of a magnetosphere. For example, Manka and Michel (1971) showed that 50% of the ⁴⁰Ar photoions, created by photoionization of the tenuous argon atmosphere, reimpact the surface of the moon, explaining the enhancement of argon in the lunar regolith (Killen 2002). At Mercury, loss of neutrals by Jeans escape and loss of photoions are both less efficient than at the moon due to Mercury’s greater mass and its magnetosphere. Thus, we expect the surface of Mercury to be enhanced in volatiles to a greater extent than the moon, even though the rate of vaporization of its surface is greater (e.g., Cintala 1992).

The fate of powdery ejecta is an important consideration. Experiments have been conducted to measure the velocity distribution of powdery ejecta from impact cratering onto sand targets (Housen, Schmidt, and Holsapple 1983; Schmidt and Holsapple 1982; Yamamoto and Nakamura 1997) and basalt targets (Gault, Shoemaker, and Moore 1963). Using the scaling formula for sand targets (Housen, Schmidt, and Holsapple 1983) for the volume of target, V_t , in units of projectile volume, ejected at $v > u$, where $u = v/v_{esc}$:

$$V_t(v > u) = 1.34(u)^{-1.22} \quad (11)$$

We conclude that the ratio of volume ejected between 0.1 v_{esc} and 1 v_{esc} to that ejected above v_{esc} is about 20. The relationship for ejection from basalt targets (Gault, Shoemaker, and Moore 1963) is a steeper function of velocity. Thus most of the ejected powder returns to the surface, while almost all of the vapor escapes from asteroids. Because the regolith is continuously bombarded by micrometeoritic material, the regolith must become devolatilized over time. Our calculations are consistent with removal of volatiles from the surfaces of asteroids and enhancement of volatiles on the surface of the moon.

Acknowledgments—R. M. Killen was supported by NASA grant NAG5-10187 from the Planetary Astronomy Program. I thank Pamela Clark for encouraging me to undertake these calculations.

Editorial Handling—Dr. Carlé Pieters

REFERENCES

- Ahrens T. J. and O’Keefe J. D. 1972. Shock melting and vaporization of lunar rocks and minerals. *Moon* 4:214–249.
- Boslough M. B. and Ahrens T. J. 1983. Shock-melting and vaporization of anorthosite and implications for an impact-origin of the moon. Proceedings, 14th Lunar and Planetary Science Conference. pp. 63–64.
- Boslough M. B., Vizgirda J., and Ahrens T. J. 1981. Shock-release of vapor from calcite. Proceedings, 12th Lunar and Planetary Science Conference. pp. 104–105.
- Chase M. W., Jr., Davies C. A., Downey J. R., Jr., Frurip D. J., McDonald R. A., and Syverud A. N. 1985. JANAF

- thermochemical tables. In *Journal of Physical and Chemical Reference Data*. Washington DC: American Institute of Physics and National Institute of Standards and Technology.
- Chen G., Tyburczy J. A., and Ahrens T. J. 1994. Shock-induced devolatilization of calcium-sulfate and implications for K-T extinctions. *Earth and Planetary Science Letters* 128:615–628.
- Cintala M. J. 1992. Impact-induced thermal effects in the lunar and Mercurian regoliths. *Journal of Geophysical Research* 97:947–973.
- Clark P. E., Killen R. M., Murphy M. E., and McCoy T. J. 2001. Examination of the apparent sulfur and other element depletions of 433 Eros relative to ordinary chondrites. Proceedings, 32nd Lunar and Planetary Science Conference.
- Ernst C. M. and Schultz P. H. 2002. Effect of velocity and angle on light intensity generated by hypervelocity. Proceedings, 33rd Lunar and Planetary Science Conference.
- Gault D. E., Shoemaker E. M., and Moore H. J. 1963. Spray ejected from the lunar surface by meteoroid impact. NASA Technical Note D-1767.
- Haskin L. and Warren P. 1991. Lunar chemistry. In *The lunar sourcebook*, edited by Heiken G., Vaniman D., and French B. V. New York: Cambridge University Press. pp. 357–474
- Hörz F. and Schaal R. B. 1981. Asteroidal agglutinate formation and the implication for asteroidal surfaces. *Icarus* 46:337–345.
- Housen K. R., Schmidt R. M., and Holsapple K. A. 1983. Crater ejecta scaling laws: Fundamental forms based on dimensional analysis. *Journal of Geophysical Research* 88:2485–2499.
- Jeanloz R. 1979. Equation of state of lunar anorthosite and anorthite: Criteria for impact melting and vaporization. Proceedings, 10th Lunar and Planetary Science Conference. pp. 622–623.
- Killen R. M. 2002. Source and maintenance of the argon atmospheres of Mercury and the Moon. *Meteoritics & Planetary Science* 37: 1223–1232.
- Killen R. M., Potter A. E., Reiff P., Sarantos M., Jackson B. V., Hick P., and Giles B. 2001. Evidence for space weather at Mercury. *Journal of Geophysical Research-Planets* 106:20509–20525.
- Lammer H., Wurz P., Patel M. R., Killen R., Kolb C., Massetti S., Orsini S., and Millo A. Forthcoming. The variability of Mercury's exosphere by particle and radiation induced surface release processes. *Icarus*.
- Lange M. A. and Ahrens T. J. 1982. The evolution of an impact generated atmosphere. *Icarus* 51:96–120.
- Love S. G. and Brownlee D. E. 1993. A direct measurement of the terrestrial mass accretion rate of cosmic dust. *Science* 262:550.
- Manka R. H. and Michel F. C. 1971. Lunar atmosphere as a source of lunar surface elements. Proceedings, 2nd Lunar and Planetary Science Conference. *Geochimica et Cosmochimica Acta* 2: 1717–1728.
- McCoy T. J. and the NEAR Science Team. 2001. The composition of 433 Eros: A mineralogical-chemical synthesis. *Meteoritics & Planetary Science* 36:1661–1672.
- Melosh H. J. 1989. *Impact cratering: A geologic process*. New York: Oxford University Press. 245 pp.
- Morgan T. H. and Killen R. M. 1998. Production mechanisms for faint but possibly detectable coronae about asteroids. *Planetary and Space Science* 46:843–850.
- Nittler L. R., Starr R. D., Lim L., McCoy T. J., Burbine T. H., Reedy R. C., Trombka J. I., Gorenstein P., Squyres S. W., Boynton W. V., McClanahan T. P., Bhangoo J. S., Clark P. E., Murphy M. E., and Killen R. M. 2001. X-Ray fluorescence measurements of the surface elemental composition of asteroid 433 Eros. *Meteoritics & Planetary Science* 36:1673–1695.
- Parfenova O. V and Yakovlev O. I. 1977. Some peculiarities of selective evaporation in target rocks after meteoritic impact. In *Impact and explosion cratering*, edited by Roddy D. J., Peppin R. O., and Merrill R. B. New York: Pergamon Press. pp. 843–859.
- Pierazzo E., Vickery A. M., and Melosh H. J. 1997. A re-evaluation of impact melt production. *Icarus* 127:408–423.
- Rubin A. E. 2002. Smyer H-chondrite impact-melt breccia and evidence for sulfur vaporization. *Geochimica et Cosmochimica Acta* 66:699–711.
- Schmidt R. M., and Holsapple K. A. 1982. Estimates of crater size for large-body impact: Gravity scaling results. Geological Society of America Special Paper 190. pp. 93–102
- Schultz P. H. 1996. Effect of impact angle on vaporization. *Journal of Geophysical Research* 101:21117–21136.
- Schultz P. H. and Gault D. E. 1990. Prolonged global catastrophes from oblique impacts. In *Global catastrophes in Earth history: An interdisciplinary conference on impacts, volcanism, and mass mortality*, edited by Sharpton V. L. and Ward P. D. Geological Society of America Special Paper 247. pp. 239–261
- Sears D. W. G., Moore S. R., Nichols S., Kareev P. H., and Benoit P. H. 2002. Intuition and experience: Asteroid surfaces, meteorites, and planetary geosciences in microgravity. *Bulletin of the American Astronomical Society* 34:841.
- Shoemaker E. 1962. Interpretation of lunar craters. In *Physics and astronomy of the Moon*, edited by Kopal Z. New York: Academic Press. pp. 283–351.
- Sugita S., Schultz P. H., and Adams M. A. 1998. Spectroscopic measurements of vapor clouds due to oblique impacts. *Journal of Geophysical Research* 103:19427–19441.
- Tyburczy J. A. and Ahrens T. J. 1993. Impact-induced devolatilization of CaSO₄ anhydrite and implications for K-T extinctions: Preliminary results. Proceedings, 24th Lunar and Planetary Science Conference. pp. 1449–1450.
- Tyburczy J. A., Frisch B., and Ahrens T. J. 1986. Shock-induced volatile loss from a carbonaceous chondrite—Implications for planetary accretion. *Earth and Planetary Science Letters* 307: 201–207.
- Yamamoto S. and Nakamura A. M. 1997. Velocity distribution of powdery ejecta. *Advances in Space Research* 20:1581–1584.